Qualitative analysis of the capillary flow stability of spurting materials by using transmitted light intensity measurements

B.M. Marín Santibañez, F. Rodríguez González, J. Pérez-González,
L.A. Vega Acosta M., and E. Moreno García
Laboratorio de Reología, Departamento de Física,
Escuela Superior de Física y Matemáticas, Instituto Politécnico Nacional,
Apartado Postal 118-209, C.P. 07051, México D.F., México

Recibido el 24 de febrero de 2003; aceptado el 19 de mayo de 2004

The stability in the capillary flow of spurting materials was analyzed by following the temporal variation of their average birefringence. Two different fluids were analyzed, a high-density polyethylene melt, and an aqueous micellar solution of Cetylpyridinium Chloride and Sodium Salicylate. Birefringence changes were detected through measurements of the transmitted light intensity and video images of the flow channel. Transmitted light intensity measurements were more sensitive and provided better information about the flow stability than pressure ones. An unstable flow region was present in the micellar solution before the onset of spurt. Also, there were periodic changes in the optical properties of both fluids, in the spurt region and at higher shear rates, which indicate that the flow is also unstable in the high shear rate branch, in contrast to the generalized assumption of the stable flow in such regime. Several frequency components of the transmitted light intensity were observed, coincident with different spurts, in the unstable flow regimes for both fluids. Finally, an outstanding decrease in the transmitted light intensity was observed in both fluids under flow conditions where slip was present.

Keywords: Flow instabilities; slip; birefringence; high-density polyethylene; micellar solutions.

La estabilidad en el flujo de Poiseuille de materiales que exhiben flujo repentino, fue analizada siguiendo la variación temporal de su birrefringencia promedio. Dos fluidos diferentes fueron analizados, un polietileno de alta densidad fundido y una solución micelar acuosa de cloruro de cetilpiridinio y salicilato de sodio. Los cambios de birrefringencia fueron detectados a través de mediciones de la intensidad de luz transmitida e imágenes de video del sistema de flujo. Las mediciones de intensidad de luz transmitida fueron más sensibles y proporcionaron mejor información acerca de la estabilidad del flujo que las de presión. Se presentó una región de flujo inestable en la solución micelar antes del inicio del flujo repentino. También, hubo cambios periódicos en las propiedades ópticas de ambos fluidos en las regiones de flujo repentino y de alta rapidez de deformación, lo cual indica que el flujo también es inestable en la rama de alto corte, en contraste con la suposición generalizada de flujo estable en ese régimen. Se observaron varias componentes de frecuencia de la intensidad de la luz transmitida, coincidentes con diferentes cambios repentinos en el flujo, en los regímenes inestables para ambos fluidos. Finalmente, se observó una notable disminución en la intensidad de la luz transmitida bajo condiciones de flujo en las que el deslizamiento estuvo presente.

Descriptores: Inestabilidades de flujo; deslizamiento; birrefringencia; polietileno de alta densidad; soluciones micelares.

PACS: 83.60.Wc; 83.80.Qr; 83.80.Sg

1. Introduction

The spurt phenomenon or stick-slip is a flow instability that manifests itself as bursts and flow rate variations in a pressure driven flow. Since the first report by Bagley and coworkers [1] of its appearance in high-density polyethylene (HDPE), the spurt phenomenon has drawn special attention because of its relevance for rheometry and polymer processing. The spurt term is sometimes found in literature when the experiments are run under controlled pressure, otherwise (controlled flow rate) this instability is called stick-slip. In most cases, both terms are used indistinctly to refer to the phenomenon that produces a sudden increase in the flow rate.

Typical spurting materials are linear polymers having a high enough ratio between the average molecular weight and the molecular weight between entanglements [2]. There are however, some more complex systems, such as wormlike micelles in solution, which have also been found to exhibit spurt under capillary flow [3-5].

There are several reviews where the main issues about the spurt or stick-slip instability are addressed [6-9]. One of the main facts occurring in the flow of a spurting material is the existence of a non-monotonic flow curve, being the instability triggered once a critical shear stress (τ_c) is reached. The non-monotonic flow curve has been roughly divided into three regions as sketched in Fig. 1. The flow is stable in the low shear rate branch (I, $\tau < \tau_c$), unstable for $\tau = \tau_c$ (II, mid shear rates), and assumed to be stable again in the high shear rate branch (III, $\tau > \tau_c$). In the case of micellar solutions however, the high shear rate branch has been scarcely explored.

Méndez-Sánchez *et al.* [5] have recently used capillary and vane rheometers to obtain the complete flow curve described in the previous paragraph, for the system of cetylpyridinium chloride 100 mmol l^{-1} /sodium salicylate 60 mmol l^{-1} (CPyCl/NaSal) in aqueous solution [10]. These authors reported more than three distinctive regions in the flow curve, as well as an apparent lack of stability in the high shear rate branch [11]. Previously, Mair and Callaghan [12] had studied the capillary flow of a similar micellar solution via rheo-nuclear magnetic resonance imaging. They suggested rapid

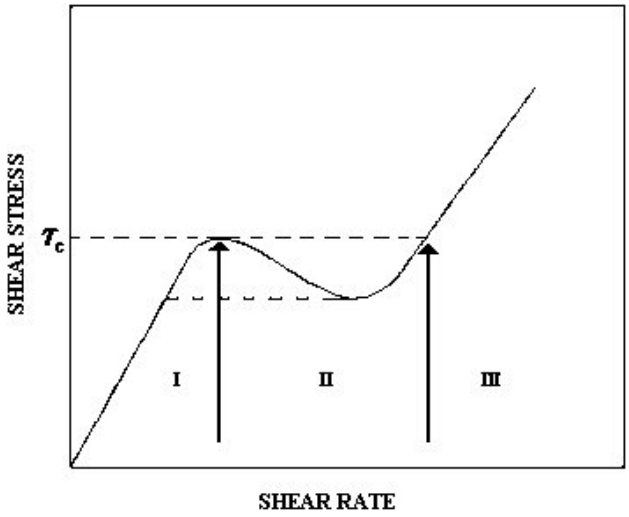

FIGURE 1. Representation of a non-monotonic flow curve.

fluctuations in velocity for shear rates at the end of the spurt region, and there was an indication of a high shear rate branch (upturn), which was not further explored. On the other hand, the flow in the low shear rate branch was reported as stable. Separately, Cappelaere *et al.* [13] used rotational rheometry and also reported steady measurements in the high shear rate branch for micellar solutions.

The spurt or stick-slip phenomenon in polymer melts has been attributed [14] to a disentanglement mechanism that occurs once the "marginal state" [15] and the τ_c are reached. However, recent measurements of oscillating electric charge in the stick-slip regime of a linear low-density polyethylene, extruded through different die materials, suggest an adhesive failure in this flow regime [16]. On the other hand, the pressure and flow oscillations occurring under controlled flow rate conditions during the stick-slip have been accepted as capacitance effects resulting from melt compressibility [9,17].

In the case of micellar solutions, it has been suggested that the system splits into shear bands of low and high shear rates whose volumetric fractions are determined by the "lever rule" [18], and that the high shear rate band is a shear-induced nematic phase [19].

In the present work, we provide a further insight into the understanding of the unstable capillary flow of spurting materials (HDPE and the CPyCl/NaSal micellar system), and their dynamics for $\tau \geq \tau_c$. Since for highly viscous solutions or melts, pressure measurements in a capillary rheometer are usually insensitive to small changes in the flow stability, we followed a different approach. It is well known that fluids containing long molecules become anisotropic under flow due to the stress field, and then exhibit birefringence. Even though it is difficult to evaluate the birefringence by using round capillaries, its evolution can be detected through measurements of the average transmitted light intensity in the flow system. These measurements are more sensitive and provide better information about the flow stability than pressure ones.

Harrison and co-workers [20] have recently pointed out some of the difficulties of using birefringence in an axisymmetric flow, which stems from the curvature of the capillary and the non-homogeneous stress distribution in this type of rheometer. In short, the transmitted light intensity through the flow system is an integration over the capillary cross section of a distribution of stresses and the consequent changes in the optical properties of the fluid along the light beam path. Thus, the capillary works as a cylindrical lens with variable refractive index because of the radial changes induced by the flow field in the optical properties of the fluid, which makes the analysis of the spatial distribution of light, and the quantitative evaluation of the stress complex.

The experimental protocol in this work was designed to favor the detection of temporal variations of the transmitted light intensity through the flow system (flow stability). Thus, the drawback mentioned in the previous paragraph is not a limitation for the present study where the evolution of the average birefringence is sufficient to assess the flow steadiness. Our analysis, in spite of being only qualitative, permits the detection of flow instabilities in the flow of transparent spurting materials. As a result, we have found that different frequency components of the transmitted light intensity were observed in the unstable flow regimes, and it is shown that a stick-slip like mechanism prevails under overspurt conditions. The details of the research are given below.

2. Experimental

The materials used in this work were a high-density polyethylene (Aldrich 42,796-9), with a reported relative density of 0.950, melt index of 0.25 gr/10 min, Mw = 125, 000, and a melting point of 130°C. In addition, the system formed by cetylpyridinium chloride 100 mmol l^{-1} /sodium salicylate 60 mmol l^{-1} (CPyCl/NaSal) in triple distilled water was chosen for the experiments. The experimental protocol for the preparation of solutions, and the production of the chemicals were the same as reported in [5,11].

The experiments with the polymer melt were run at a temperature of 180°C in a PL 2100 Brabender single screw extruder, of 3/4" in diameter and length to diameter ratio (L/D) of 25/1; meanwhile, those with the micellar solution were performed at 25°C with a pressure controlled capillary rheometer. The pressure drop between capillary ends was measured with a Dynisco® pressure transducer in the polymer melt and a Validyne® one in the solution. The flow rates in both cases were determined by collecting and measuring the ejected mass as a function of time.

Duran® borosilicate glass capillaries of length to diameter ratio of (L/D) of 20 (D = 0.17 cm) and 400 (D = 0.29 cm), were used for the experiments with the melt and the solution, respectively.

Average birefringence changes were detected through measurements of the transmitted light intensity and video images of the flow channel using a traditional configuration of crossed polarizers and a He-Ne laser with λ = 633 nm

(see Fig. 2). The transmitted light intensity was measured and stored in real time, at a rate of 10 points/s, with a photoresistor and a data acquisition board coupled to a PC via a LabView® program, respectively. The photoresistor works in such a way, that an increase of the light intensity produces a decrease in the measured resistance and voltage, and vice versa, according to the Ohm's law. Thus, a constant current of 0.1 mA was supplied, so as not to allow saturation of the measuring voltage (5 V). The light beam was sent through a 9 mm of a focal distance lens, and the illuminated field covered an observation window of about 1.3 centimeters in length. For the HDPE the observation window was set around the mid-length of the capillary and at around 35 diameters from the exit in the case of the solution. The transmitted light field was then focused onto the detector, making sure that the projected image always lied inside the area of detection. This was particularly relevant in the study of the polymer melt, since the natural movement of the extruder produced small changes in the vertical position of the flow channel image. Thus, we made sure that variations in the detected signal were not an artifact and resulted from real changes in the flow conditions. In our experiments, the image is inverted, and appears amplified in a bigger proportion in the vertical direction because of the differences in the refractive indexes between the used fluids and the capillary.

3. Results and analysis

The wall shear stress (τ_w) and the apparent shear rate ($\dot{\gamma}$) were calculated using $\tau_w{=}(D\Delta p)/4L$ and $\dot{\gamma}_{app}{=}(32Q)/(\pi D^3)$, respectively, where Δp is the pressure drop between capillary ends, and Q is the volumetric flow rate.

3.1. High-density polyethylene

The flow curve for the HDPE at T = 180°C is shown in Fig. 3, which displays the characteristic shape of a non-monotonic

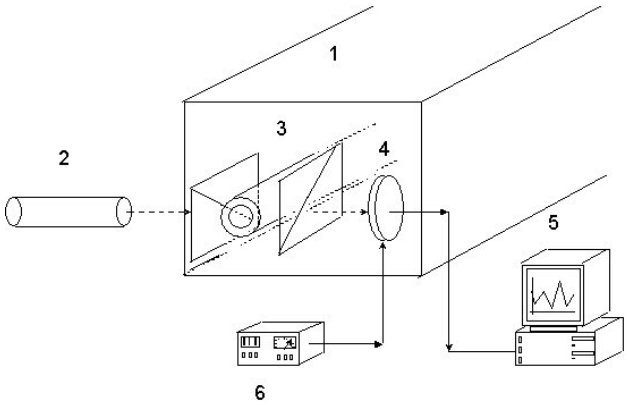

FIGURE 2. Schematic diagram of the experimental set up. 1) Extruder or water bath; 2) He-Ne laser; 3) Polarizers; 4) Photoresistance; 5) Personal computer; 6) Current supply.

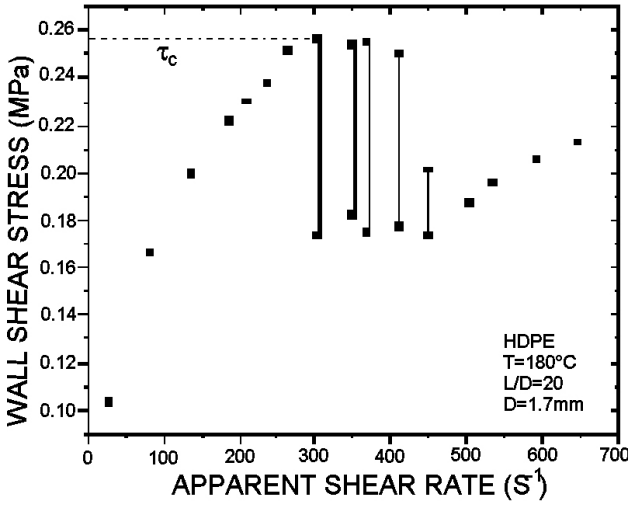

FIGURE 3. Flow curve for HDPE obtained with a glass die at T = 180°C. Vertical lines and double points represent the amplitude of pressure oscillations.

relationship between the shear stress and the shear rate (compare with Fig. 1), being the unstable oscillating flow or stick-slip triggered at a critical shear stress of the order of 0.26 MPa. While the oscillating region at mid shear rates is evident, pressure measurements did not suggest an unstable behavior under overspurt conditions.

Measurements of the transmitted light intensity as a function of time were performed for each point in Fig. 3. The average values of the light intensity (voltage), and some of their corresponding video images are shown in Figs. 4 and 5a-f, respectively; meanwhile voltage changes with time are shown in Figs. 6a-f for some shear rates.

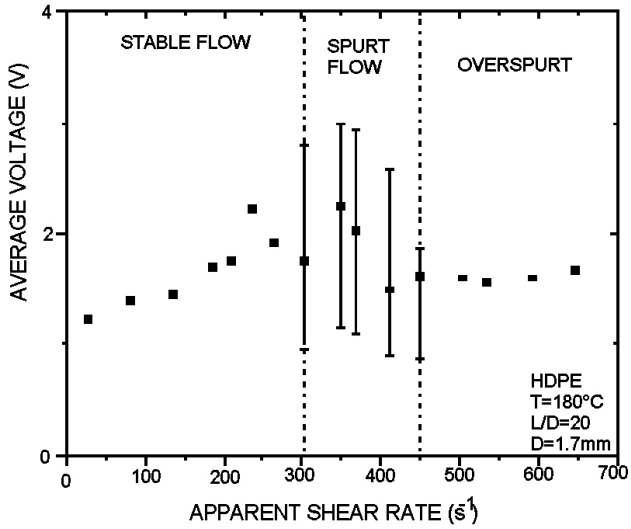

FIGURE 4. Average voltage values as a function of the apparent shear rate for HPDE.

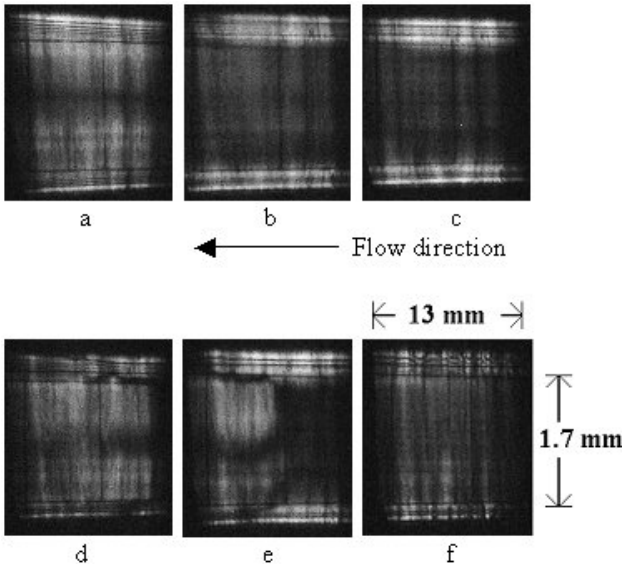

FIGURE 5. Images of the flow channel between crossed polarizers for different flow conditions in HDPE; a) 30.1 s^{-1}, b) 212.6 s^{-1}, c) 305.1 s^{-1}, d) 370.7 s^{-1}, e) 412.6 s^{-1}, f) 537.3 s^{-1}.

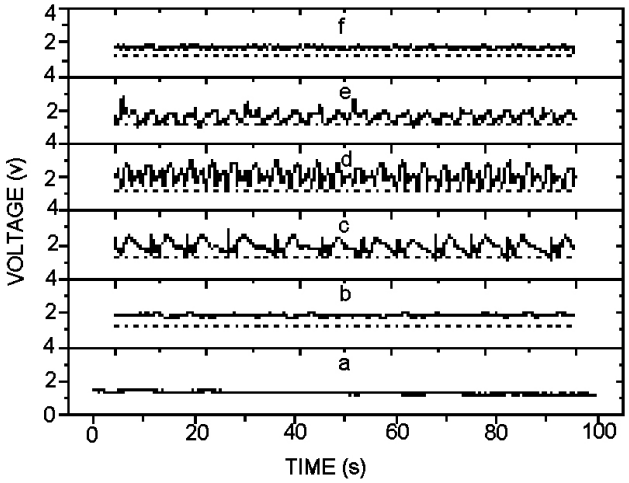

FIGURE 6. Variations in voltage (transmitted light intensity) in HDPE as a function of time for different apparent shear rates; a) 30.1 s^{-1}, b) 212.6 s^{-1}, c) 305.1 s^{-1}, d) 370.7 s^{-1}, e) 412.6 s^{-1}, f) 537.3 s^{-1}. The horizontal dashed line in all figures represents the average transmitted light intensity for the smallest shear rate (a). It is included for comparison purposes.

Results in Figs. 4 and 5a-f show that the transmitted light intensity decreased (voltage increased) as the shear rate was increased up to the onset of the oscillating flow (see below), in which the transmitted light also oscillated. Then, under overspurt conditions, there was an increase in the transmitted light intensity with respect to the previous flow regime and a further apparent asymptotic value. It is outstanding, that the transmitted light decreased with increasing shear rate in the stable flow regime, since a higher orientation of the macromolecules is expected along with the shear rate. Although this fact needs to be verified using a different flow cell in which the stress distribution is simpler, the decrease in the transmitted light intensity appeared at shear rates for which slip at the capillary wall has been reported [21], and this trend is perhaps a signature of such phenomenon. Furthermore, the decrease in the transmitted light intensity was coincident with the appearance of electrostatic charge on the surface of the extrudate, which is an indication of a slip at the die wall [16]. The presence of a slip at the wall would decrease the shear rate in the bulk, and produce therefore, a decrease in the orientation of the molecules, as well as in the average birefringence, according to the observation in this work.

On the other hand, it is observed in Fig. 6a that the voltage for the lowest shear rate was almost constant, while not significant variations in pressure drop were detected. As the wall shear stress approached to the critical for the stick-slip, a low-amplitude oscillation appeared (6b). As soon as the critical stress for spurt was reached, there was a dramatic change in the polymer birefringence and the intensity of the detected light oscillated with different frequency components (6c-e), which means that material with different optical properties is passing alternatively through the observation window. In contrast to the observed for $\tau < \tau_c$, the amplitude of the voltage oscillations in the stick-slip was comparable to the average value for each apparent shear rate, and the transmitted light intensity decreased during the spurts (represented by the shorter periods), suggesting that less oriented material is passing through the observation window. This observation is consistent with material slipping at the wall during the spurts [16,21].

As seen from Fig. 6f, at shear rates beyond the oscillating region, under overspurt conditions, most of the oscillation components disappeared remaining only one with higher frequency. Also, the amplitude of the oscillation decreased as compared to the observed in the stick-slip regime. Again, it is evident that the alternation of fluid with different optical properties is passing more often through the observation window. This is an interesting result, which is in contrast with the common assumption that the flow is stable in the high shear rate branch. In other words, it seems that a stick-slip like mechanism prevails under overspurt conditions, and that once the instability starts at τ_c, the flow is never stable again.

From the previous results, it is evident that the birefringence changes reflect temporal variations in the flow. Even though we were unable to register simultaneously the evolution of pressure and light intensity in the stick-slip, we were able to relate the birefringence changes with different spurts. Such spurts became evident as surface defects on the extrudates and represent different frequency components of the pressure drop for a given shear rate (Fig. 7). Note that at least two different distortions with similar periods are evident in the extrudate in Fig. 7, their values of 7.61 and 7.59 s were obtained from the signal in Fig. 6c.

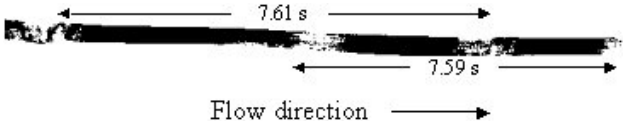

FIGURE 7. Photograph of an extrudate of HDPE obtained in the stick-slip regime at an apparent shear rate of 305.1 s^{-1}. Note the two different periodic distortions, which are related to pressure oscillations whose periods are 7.61 and 7.59 s.

A sequence of images taken during the stick-slip and their corresponding cycles are shown in Fig. 8. Because of the complex distribution of the birefringence in the capillary we will not attempt to explain the spatial distribution of the light, but it is noteworthy the alternation of clear and dark regions, which reflects changes in the fluid structure, as well as the unsteadiness of the flow. As far as we know, there are no reports of the existence of different frequency components of the pressure oscillations for a given shear rate in the stick-slip regime of HDPE melts. Robert *et al.* [22], recently reported the existence of more than one single oscillation frequency in HDPE, but such observation was made in an uncommon second unstable region. The analysis of the stick-slip phenomenon has been performed assuming the existence of a single pressure frequency for a given shear rate [17]. However, the results in the present work suggest that the stick-slip phenomenon is more complex than it is usually thought, and the existence of different pressure oscillations should be considered for a better description of the phenomenon.

3.2. Micellar solution

The flow curve for the micellar solution at 25°C is shown in Fig. 9, in which a non-monotonic relation between the shear stress and the apparent shear rate is also evident. The spurt phenomenon is observed at a critical shear stress (τ_c) of the order of 15 Pa, and three different slopes are visible in the flow curve for $\tau < \tau_c$. Méndez-Sánchez and co-workers [5] suggested the region between 0.4 and 1.2 s^{-1} as unstable because of very small fluctuations in the pressure drop, as well as in the shear rate. Similar to the observed in the experiments with the melt, the spurt region at mid shear rates is evident, and pressure measurements did not suggest an unstable behavior for shear rates beyond the upturn ($\tau > \tau_c$).

The transmitted light intensity was measured as a function of time for several shear stress values of the flow curve in Fig. 9. The results of the transmitted light intensity measurements are shown in Figs. 10a-f.

From the results in Figs. 10a-f, it is observed that the voltage (transmitted light) at rest (a), and for the lowest shear rate (b) was almost constant. There was however, an increase of the transmitted light intensity as soon as the flow started (region I), which suggests an orientation of the micelles in the flow direction (b). For shear rates in region II of Fig. 9, there was a marked change in the slope of the flow curve and a low amplitude oscillation of the light intensity (c), in agreement with the lack of stability suggested by Méndez-Sánchez

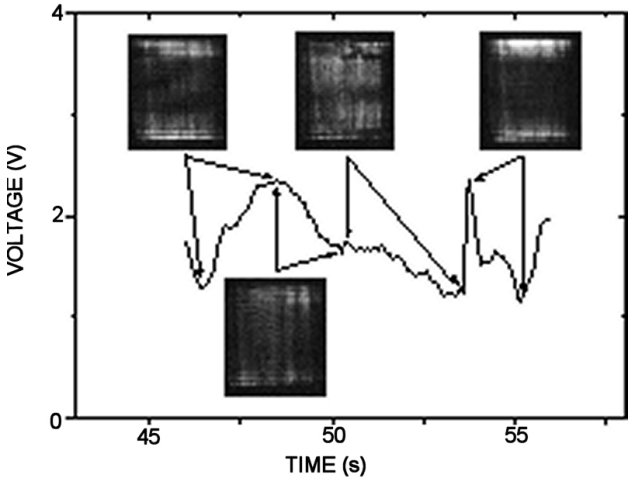

FIGURE 8. Images of the flow channel between crossed polarizers during a stick-slip cycle in HDPE at an average apparent shear rate of 305.1 s^{-1}.

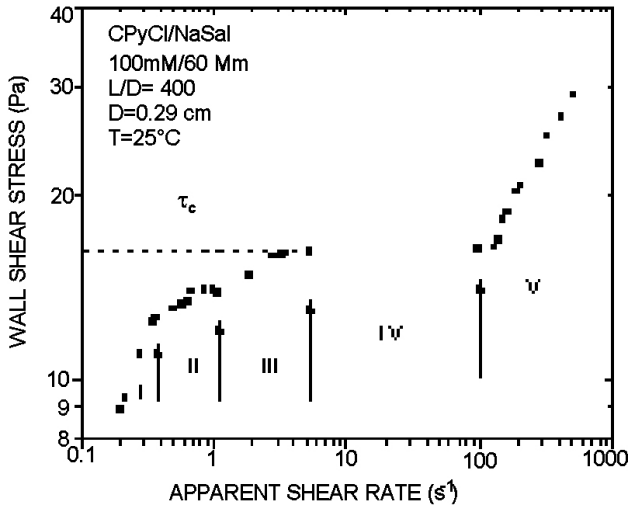

FIGURE 9. Flow curve for CPyCl/NaSal.

et al. [5] for this flow regime. At higher shear stresses (region III), the birefringence was stable again up to the onset of spurt (d). Then, there was a jump of one order of magnitude in the shear rate once spurt was triggered (region IV). The transient for the flow to occur in the high shear rate branch was of the order of a few minutes.

Once the flow occurred in the high shear rate branch (region V), significant pressure variations were not observed, but different frequency components with increased light intensity appeared (Figs. 10e and 10f). These new patterns became faster with greater amplitude as the shear stress was further increased; they resemble the stick-slip behavior observed for the HDPE, even though the physical mechanism driving the instabilities may be different in both cases. This sort of behavior, however, is unexpected considering that the experiments were run under controlled pressure.

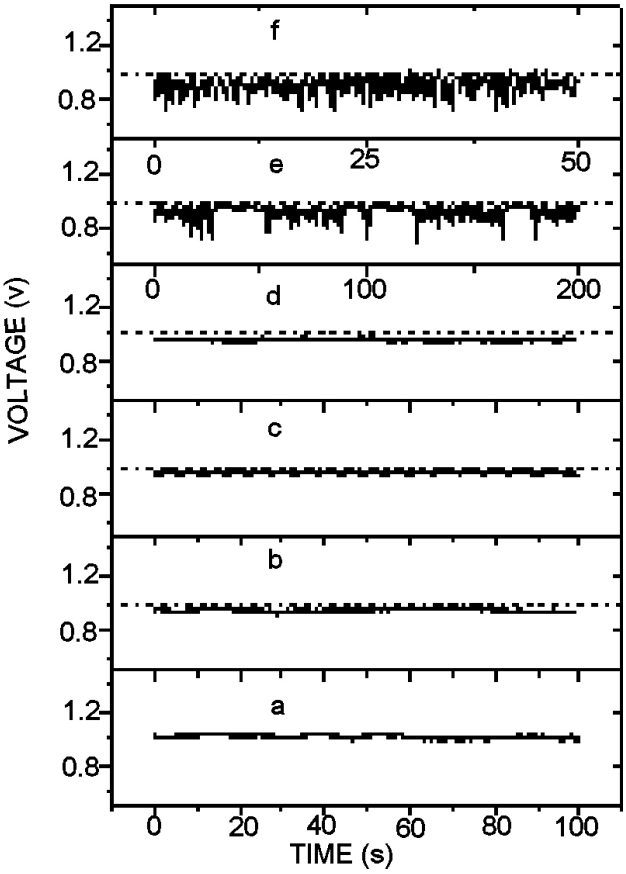

FIGURE 10. Variations in voltage (transmitted light intensity) in CPyCl/NaSal as a function of time for different apparent shear rates; a) rest, b) 0.37 s^{-1}, c) 0.69 s^{-1}, d) 1.88 s^{-1}, e) 101 s^{-1}, f) 168 s^{-1}. The horizontal dashed line in all figures represents the average transmitted light intensity at rest (a). It is included for comparison purposes.

In the high shear rate branch, video images exhibited periodically small volumes of material with increased and decreased light intensity (more or less orientation), which were traveling in the flow direction, as observed in the HPDE. It must be pointed out, however, that the transmitted light intensity decreased during the spurts in the melt, but increased in the micellar solution (see Figs. 6 and 10). This is likely related to the physical mechanism responsible for the instability in each case, disentanglement (apparent slip) in the melt [14], and shear banding in the micellar system [18,23].

The results in the previous paragraphs clearly show that for this micellar solution the flow is also unstable under overspurt conditions. To our knowledge, this is a pioneer report on the stability of the flow in the high shear rate branch for micellar solutions.

A further analysis of the signals of the transmitted light intensity in Figs. 10a-f, and the video images showed that there is a "base line" of minimum transmitted light intensity, from which the last increases during the oscillations. It is interesting to note that there is a decrease in the transmitted light intensity in region II with respect to region I, which is accompanied by a decrease in the slope of the flow curve in Fig. 9. In a similar way to the observed with the HDPE, this bending of the flow curve may be attributed to a flow enhancement or apparent slip, and the average decrease in the light intensity might also be considered as a signature of this phenomenon. We have recently obtained the velocity profiles for the same CPyCl/NaSal system [23], and they show an apparent slip in region II of the flow curve, which is consistent with the decrease in the transmitted light intensity observed in this work.

Finally, it is noteworthy that, although it is not included in this work, we have also observed the unstable flow in the high shear rate branch, and the decrease in the transmitted light intensity under slip flow for a micellar solution of cetyltrimethylammonium bromide and sodium salicylate, as well as in two linear low-density polyethylenes, which indicates that these phenomena are ubiquitous of spurting materials. It is likely that the instability is originated, in both cases, at the die entrance as suggested by observations with the micellar solution at different positions along the capillary (see also Ref. 24).

4. Conclusions

The capillary flow of two spurting materials was studied in this work using birefringence. Measurements of the transmitted light intensity provided better information about the flow stability than pressure ones. An unstable flow regime was detected in the micellar solution before the onset of spurt, and it was found that the flow was unstable in the high shear rate branch for both fluids, in contrast to the common assumption of stable flow in such a flow regime. Several frequency components of the transmitted light intensity were observed in the unstable flow regimes for both fluids, consistent with the alternation of fluid with different optical properties passing through the observation window. Finally, a decrease in the transmitted light intensity was observed for both fluids under flow conditions where slip was present.

As a closure, it is necessary to point out the limitation of the experimental procedure used in this work, which only allows to obtain qualitative information about the unstable flow regions. Future work should include a quantitative evaluation of birefringence and its relation to the shear stress by using a flow geometry with constant optical path.

Acknowledgements

This research was supported by CGPI-IPN (20010565) and CONACYT (34971-U). B.M. M-S and F.R-G had PIFI and CONACYT scholarships. J. P-G, L.deV and E. M-G are COFFA-EDI-EDD fellows. We acknowledge the reviewers for very useful comments.

1. E.B. Bagley, I.M. Cabot, and D.C. West, *J. Appl. Phys.* **29** (1958) 109.
2. Y.H. Lin, *J. Rheol.* **29** (1985) 605.
3. P.T. Callaghan, E.M. Cates, C.J. Rofe, and J.B.A.F. Smeulders J., *Phys. II* (France) **6** (1996) 375.
4. S. Hernández-Acosta, A. González-Alvárez, O. Manero, A.F. Méndez-Sánchez, J. Pérez-González, and L. de Vargas L., *J. Non-Newtonian Fluid Mech.* **85** (1999) 229.
5. A.F. Méndez-Sánchez, M.R. López-González, V.H. Rólon-Garrido, J. Pérez-González, and L. de Vargas, *Rheol. Acta* **42** (2003) 56.
6. C.J.S. Petrie and M.M. Denn, *AICHE Journal* **22** (1976) 209.
7. G.V. Vinogradov, V.P. Protasov, and K.E. Dreval, *Rheol. Acta* **34** (1984) 495.
8. Y.M. Joshi, A.K. Lele, and R.A. Mashelkar, *J. Non-Newtonian Fluid Mech.* **89** (2000) 303.
9. M.M. Denn, *Ann. Rev. Fluid Mech.* **33** (2001) 265.
10. H. Rehage and H. Hoffmann, *Mol. Physics* **74** (1991) 933.
11. V.H. Rolón-Garrido, J. Pérez-González, and L. Vega Acosta Montalban, *Rev. Mex. Fis.* **49** (2003) 40.
12. R.W. Mair and P.T. Callaghan, *J. Rheol.* **41** (1997) 901.
13. E. Cappelaere, J.F. Berret, J.P. Decruppe, R. Cressely, and P. Lindner, *Phys. Rev. E.* **56** (1997) 1869.
14. S.Q Wang, *Adv. Polym. Sci.* **138** (1999) 227.
15. F. Brochard and P.G. De Gennes, *Langmuir* **8** (1992) 3033.
16. J. Pérez-González, *J. Rheol.* **45** (2001) 845.
17. C.F.J den Doelder, R.J. Koopmans, and J. Molenaar, *J. Non-Newton. Fluid Mech.* **79** (1998) 503.
18. N.A. Spenley, X.F. Yuan XF, and M.E. Cates, *J. Phys. II* (France) **6** (1996) 551.
19. J.F. Berret, *Langmuir* **13** (1997) 2227.
20. P. Harrison, L.J.P. Jansen, V.P. Navez, G.W.M. Peters, and F.P.T. Baaijens, *Rheol. Acta* 41 (2002) 114.
21. H. Münstedt, M. Schmidt, and E. Wassner, *J. Rheol.* **44** (2000) 413.
22. L. Robert, B. Vergnes, and Y. Demay, *J. Rheol.* **44** (2000) 1183.
23. A.F. Méndez-Sánchez *et al., J. Rheol.***47** (2003) 1455.
24. J. Pérez-González, L. Pérez-Trejo, L. de Vargas, and O. Manero, *Rheol. Acta* **36** (1997) 677